
Topographic Assessment of Periodontal Craters and Furcation Involvements by Using 2D Digital Images Versus 3D Cone Beam CT: an in-vitro Study

Bart Vandenberghe¹, Reinhilde Jacobs², Jie YANG³

Objective: To validate two-dimensional (2D) digital intraoral and three-dimensional (3D) cone beam CT (CBCT) images in assessment of periodontal bone craters and furcation involvements.

Methods: Forty-one periodontal bone defects of human skulls were evaluated using intraoral digital radiography and CBCT. Digital radiographs were made with a size #2 CCD sensor and a 60 kV DC X-ray unit, with a 0.28 mAs exposure setting. For CBCT, jaw bone images were obtained at 120 kV and 23.87 mAs. Periodontal bone craters and furcation involvements on both imaging modalities were assessed and compared with the gold standard, the direct skull observation.

Results: Detection of both craters and furcation involvements was improved significantly by using 3D CBCT images ($p = 0.374$ and $p = 1.000$ respectively) than by 2D intraoral CCD images ($p = 0.001$ and $p = 0.006$ respectively), when compared with the gold standard. 2D images had a failure rate of 31% and 42% for detection of craters and furcation involvements. In contrast there was 100% detection with 3D CBCT. For crater assessment, 2D images overestimated in 62% of sites and underestimated in 13% of sites. CBCT showed 88% accurate classifications, and 12% overestimations. For furcation involvements, only 25% were correctly classified from the 2D digital images. CBCT images allowed correct classification 100% of the time. Distinctions between the vestibular and oral bony defects were only marked on CBCT images.

Conclusion: CBCT demonstrated more potential in the morphological description of periodontal bone craters and furcation involvements than 2D intraoral images. The latter mostly overestimated the defects or showed insufficient information of the bone defects. These findings may be useful for further studies on periodontal diagnosis using CBCT.

Key words: cone beam CT, crater, furcation involvement, intraoral radiography, jaw bone, periodontium

¹ PhD and MS Student, Oral Imaging Centre, School of Dentistry, Oral Pathology and Maxillofacial Surgery, Faculty of Medicine, Katholieke Universiteit Leuven, Leuven, Belgium, & Division of Oral and Maxillofacial Radiology, Temple University School of Dentistry, Philadelphia, USA.

² Professor and Head of Oral Imaging Centre, School of Dentistry, Oral Pathology and Maxillofacial Surgery, Faculty of Medicine, Katholieke Universiteit Leuven, Leuven, Belgium.

³ Director and Associate Professor, Division of Oral and Maxillofacial Radiology, Temple University School of Dentistry, and Associate Professor, Department of Diagnostic Imaging, Temple University School of Medicine, Philadelphia, USA.

Corresponding author: Dr. Jie YANG, Division of Oral and Maxillofacial Radiology, Temple University School of Dentistry, Philadelphia, Pennsylvania 19140, USA. Tel: 215-707-1579. Fax: 215-707-5719. E-mail: jie.yang@temple.edu

Currently, clinical probing and intraoral radiography are the main diagnostic tools for periodontal diseases. However, studies have shown limitations for both techniques in assessment of periodontal bone loss¹⁻¹¹. The major limitation or drawback is that neither technique provides valid three-dimensional (3D) information for assessment as well as classification of periodontal bone defects, especially infrabony defects and furcation involvements. The infrabony defects are also referred to as bony craters*, which are usually saucer-

* For descriptions of bony defects, the general term crater is used in this article, which can refer to 1-walled, 2-walled, 3-walled or 4-walled defects or any combination of these.

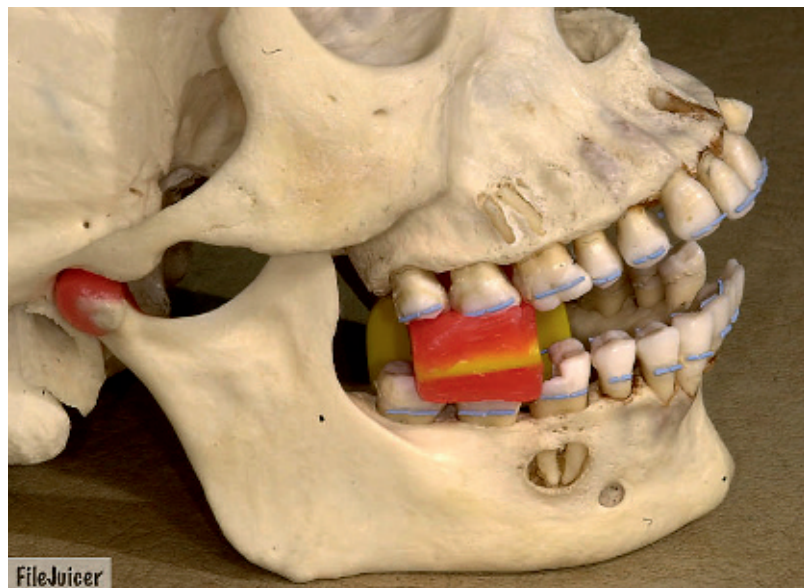


Fig 1 Standardised exposure set-up: dry skull with gutta-percha markers (for linear bone loss assessment in our preceding study) and waxed imprints before covering the jaws with soft tissue substitute. Non linear defects were present around almost all teeth. A clearly visible defect is seen on the third maxillary molar.

shaped with 3 or 4 bony walls remaining. Furcation involvements refer to the periodontal defects among the multi-rooted teeth where roots diverge. Correct interpretations of these bony defects are crucial to predict prognoses of periodontally affected teeth as well as to make correct treatment planning⁸⁻²². Different types and degrees of the bone defects often require different treatment procedures^{23,24}. Because of the limitations of the existing methods and the 3D nature of many periodontal bone defects, the current diagnostic approach needs further improvement⁸⁻¹¹.

Cone beam computed tomography (CBCT, or dental CT) is a recently developed imaging modality. It can provide 3D information of dentition as well as its supporting structures. Compared with conventional CT, CBCT considerably reduces radiation exposure to patients²⁵⁻²⁷. Application of this new imaging modality in addition to existing 2D digital intraoral radiographs may offer new perspectives on periodontal diagnosis and treatment planning^{14,15,28}.

The purpose of the present study was to explore the diagnostic value of CBCT in the determination and classification of the 3D topography of periodontal bone craters and furcation involvements. We hypothesised that CBCT would allow more accurate assessment of the periodontal bone defects than intraoral radiography. The present study was a continuation of our previous research on assessment of linear bone loss with CBCT¹⁵.

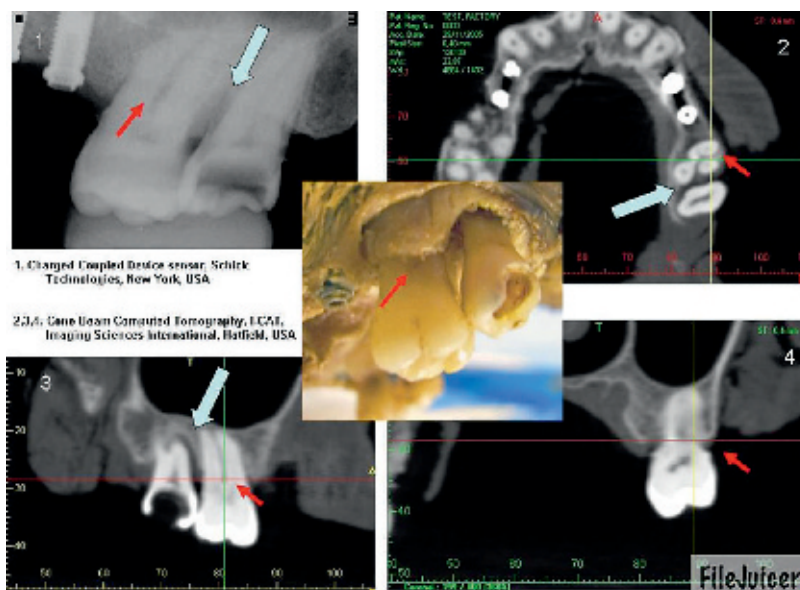
Materials and Methods

Forty-one periodontal bony defects, 19 bony craters and 22 furcation involvements, from two adult human skulls, a cadaver head and a dry skull, were evaluated using intraoral digital radiography (charged coupled device (CCD) sensor, Schick Technologies, NY, USA) and CBCT (I-Cat, 12 bit, Imaging Sciences International, Hatfield, PA, USA). The maxilla and mandible of the cadaver head were fixed with 10% formalin and used as the clinical subject. The adult human dry skull was covered with a soft tissue substitute, Mix D²⁹, and used as a simulation.

For the intraoral protocol, images were obtained with a size #2 CCD intraoral digital sensor and a direct current (DC) X-ray unit (Heliodent DS, Sirona Dental Systems LLC, Charlotte, USA) combined with a rectangular (4 cm x 3 cm) collimator (Universal Collimator, RINN Corporation, Illinois, USA). The focal-film distance was 30 cm. The paralleling technique was applied in a standardised exposure set-up with film holding system (XCP, RINN Corporation, Illinois, USA) and standardised bite blocks (Fig 1). The exposure setting was 60 kVp with 0.28 mAs (40 ms x 7 mA).

For CBCT scanning, the occlusal plane of the jaw bones was positioned horizontally to the scan plane and the midsagittal plane was centred. The field of view (FOV) or the beam diameter at the surface of the image receptor (beam height) was adjustable and set to visu-

Fig 2 Digital X-ray images of molar region from the cadaver maxilla. 1) Two-dimensional CCD image; 2) CBCT axial slice; 3) CBCT coronal slice; and 4) CBCT panoramic view (oblique). Observers described the defects using both imaging modalities (CCD and CBCT) and comparison was made to the gold standard, which was obtained after removing the soft tissues (centre). The small arrows indicate a furcation involvement that was overestimated by the three observers on the 2D CCD radiograph. The larger arrows indicate a mesial 3-walled periodontal bone defect that was marked as 1-walled on the 2D CCD image.



alise the entire jaws, giving between 54 and 159 slices of 0.4 mm thickness (between approximately 20 mm and 60 mm beam height). Images were obtained using a low-dose protocol, of 120 kVp and 23.87 mAs with a typical voxel size of 0.4 mm (Fig 2).

Assessment of the periodontal bony defects using both imaging modalities was by three observers (a post-graduate student in radiology and two radiology faculty members, Temple University School of Dentistry, Philadelphia, USA). Each of them in turn viewed the images in a darkened room on a notebook with 17 inch LCD monitor and high screen resolution (1440 x 900 pixels). Intraoral 2D images were displayed with the Emago advanced, V.3.5.2 software in Tagged Image File Format (TIFF). Dedicated filtering and grey scale enhancement methods were allowed to analyse the selected sites. CBCT images were viewed with the I-CAT software (Xoran CAT V.2.0.21, Xoran Technologies Inc. Michigan, USA, 2005). Analysis was carried out using coronal, sagittal and axial slices of 0.4 mm each, for the selected teeth. Measurement tools on both programs were used for furcation classification.

A group of 10 teeth in the molar region of the maxilla and mandible, containing 41 sites, including mesial and distal 3D crater defects and vestibular and oral (for maxillary molars vestibular, mesial and distal) furcation involvements, was selected for comparison and statistical analysis. Physical descriptions on the skull models were considered as the gold standards for further accu-

racy assessment of both imaging modalities. For the cadaver jaws, the gold standard was obtained after image acquisition, by flap surgery to allow physical description and classification. Furcation classification was carried out using a periodontal probe. For the dry skull, the gold standard was obtained prior to adding soft tissue substitute and image acquisition.

Statistical analysis

Bone defects and crater involvements of the selected sites, observed on the digital intraoral and CBCT images, were compared with the gold standard. Imaging methods and observers were used as independent variables and bone defects and furcation involvements as the dependent variables. The latter were classified by an ordinal scale from 0 to 4 (no defect, 1-walled, 2-walled, 3-walled and 4-walled) and from 0 to 3 (no furcation involvement, class I, class II and class III) respectively. The gold standard was obtained by averaging the scores of two observers. Intra-class correlation showed no observer effect for these scores.

Because of the ordinal nature of the acquired data, nonparametric statistics were used for the analyses^{30,31}. The observer effect for both dependent variables was tested with the Kruskal-Wallis test and showed no significant difference among the three observers ($p > 0.05$). A 50% repeat of measurements was done at an interval of one week and a high reliability was found amongst every observer (interval of 0.986-0.997 with 95% con-

TABLE 1 Crater assessment: gold standard versus CCD and CBCT assessment. The ordinal scale represents classifications (0-, 1-, 2-, 3- and 4-walled defects). Results are the averaged values of three observers. For CCD, only 25% of the craters matched the gold standard compared to 88% for CBCT

Crater	Gold standard	2D CCD	3D CBCT
Mandibular right first molar mesial	0	0	0
Mandibular right first molar distal	2	2	2
Mandibular right second molar mesial	0	0	0
Mandibular right second molar distal	3	0	3
Mandibular right third molar mesial	0	0	0
Maxillary right first molar mesial	3	1	3
Maxillary right first molar distal	3	0	3
Maxillary right second molar mesial	2	1	2
Maxillary right second molar distal	2	2	1
Maxillary right third molar mesial	2	0	2
Maxillary right third molar distal	2	0	2
Mandibular left first molar mesial	2	2	2
Mandibular left first molar distal	1	2	1
Mandibular left second molar mesial	3	0	2
Mandibular left second molar distal	3	1	3
Maxillary left second molar mesial	3	3	3
Maxillary left second molar distal	2	1	2
Maxillary left third molar mesial	3	1	3
Maxillary left third molar distal	1	2	1

TABLE 2 Kruskal-Wallis test and Mann-Whitney test for accuracy assessment of the two imaging techniques. The 2D intraoral technique was significantly different from the gold standard for both dependent variables. The significant differences between both 2D and 3D images showed more accurate assessment of craters and furcation involvements by the 3D CBCT images

Mann-Whitney test				Kruskal-Wallis test		
Crater	Z	GS vs 2D CCD	GS vs 3D CBCT	2D CCD vs 3D CBCT	χ^2 value	GS vs 2D CCD vs 3D CBCT
	Exact Sig.	-3.264 0.001	-0.471 0.374	-2.950 0.002	Df	13.387 2
					Exact Sig.	0.001
Furcation	Z	-0.430	0.000	-0.430	χ^2 value	0.269
	Exact Sig.	0.322	0.608	0.322	Df	2
					Exact Sig.	0.892

fidence and a single measure intra-class correlation coefficient of 0.987). Those measurements were then averaged for further calculations (see Table 1).

The Kruskal-Wallis test³¹ was used to compare the gold standard with 2D intraoral and 3D CBCT images in assessment of the periodontal bone defects. The statistical analyses were done with SPSS V.13.0 statistical software (SPSS In., Chicago, USA).

Results

Craters

Table 1 is a summary of the observations of the selected crater sites. The gold standard versus 2D intraoral digital imaging and 3D CBCT assessment of the crater sites and their mean values are shown. The 0 values in the gold standard, representing absence of craters and furcation involvements, were excluded from the statistical analy-

TABLE 3 Furcation assessment: gold standard versus CCD and CBCT assessment. Classification in main classes is given (0 = no defect, 1/2/3 = class IA/IB/IC, 4/5/6 = class IIA/IIB/IIC, 7/8/9 = class IIIA/IIIB/IIIC). Averaged values of three observers are shown. Subclasses were not used in statistical analyses because of the nature of the ordinal scale. Of the furcation involvements, 58% were detectable with the CCD technique and only 25% of them were correctly classified. In contrast, CBCT allowed 100% detection and correct classification of furcation involvements

Furcation	Gold standard	2D CCD	3D CBCT
Mandibular right first molar vestibular	1	7	1
Mandibular right first molar oral	4	7	4
Mandibular right second molar vestibular	0	0	0
Mandibular right second molar oral	0	0	0
Mandibular right third molar vestibular	0	0	0
Mandibular right third molar oral	0	0	0
Maxillary right first molar mesial	1	0	1
Maxillary right first molar distal	0	0	0
Maxillary right first molar vestibular	1	0	1
Maxillary right second molar mesial	0	0	0
Maxillary right second molar distal	0	0	0
Maxillary right second molar vestibular	1	0	1
Mandibular left first molar vestibular	0	0	0
Mandibular left first molar oral	1	1	1
Mandibular left second molar vestibular	0	0	0
Mandibular left second molar oral	4	0	4
Maxillary left second molar mesial	1	4	1
Maxillary left second molar distal	7	7	7
Maxillary left second molar vestibular	1	7	1
Maxillary left third molar mesial	0	0	0
Maxillary left third molar distal	1	0	1
Maxillary left third molar vestibular	1	1	1

ses as no different values were scored with both techniques, thus yielding 100% specificity for this variable for 2D and 3D imaging.

The gold standard versus 2D digital intraoral images and 3D CBCT were compared using the Kruskal-Wallis test. There was a significant difference ($p = 0.001$) between the gold standard and the imaging modalities. Further assessment through the Mann-Whitney test showed that this was due to the 2D intraoral imaging technique, which was significantly different from the gold standard ($p = 0.001$; Table 2). Table 2 also demonstrated the significant difference ($p = 0.002$) between the 2D and the 3D imaging techniques in assessment of craters. Fig 3a is a graphic representation of the values in Table 1, showing frequency counts of gold standard, 2D CCD and 3D CBCT images.

From the results in Table 1, we found that for intraoral digital imaging, 31% of the defects were not detected. Only 25% of the observations had the same class as

the gold standards. A tendency to overestimate the crater involvement was seen in 62% of the sites and only 13% were underestimations. For CBCT however, all crater involvements were visible. Observations deviated only slightly: 12% were overestimations and 88% were classified correctly. We found no significant difference between the gold standard and the 3D imaging modality ($p = 0.374$, Table 2).

Furcation involvement

Table 3 shows the observations of the selected furcation sites. The ordinal scale was adjusted to a 0 to 3 scale (see Fig 3b) for statistical analyses. Again the 0 values of the gold standard were excluded from the statistical analyses. However, for this variable, the Kruskal-Wallis test and subsequently the Mann-Whitney test revealed no significant differences among the gold standard and two imaging modalities. Hence, the data of both variables were explored and revealed normal variations in the me-

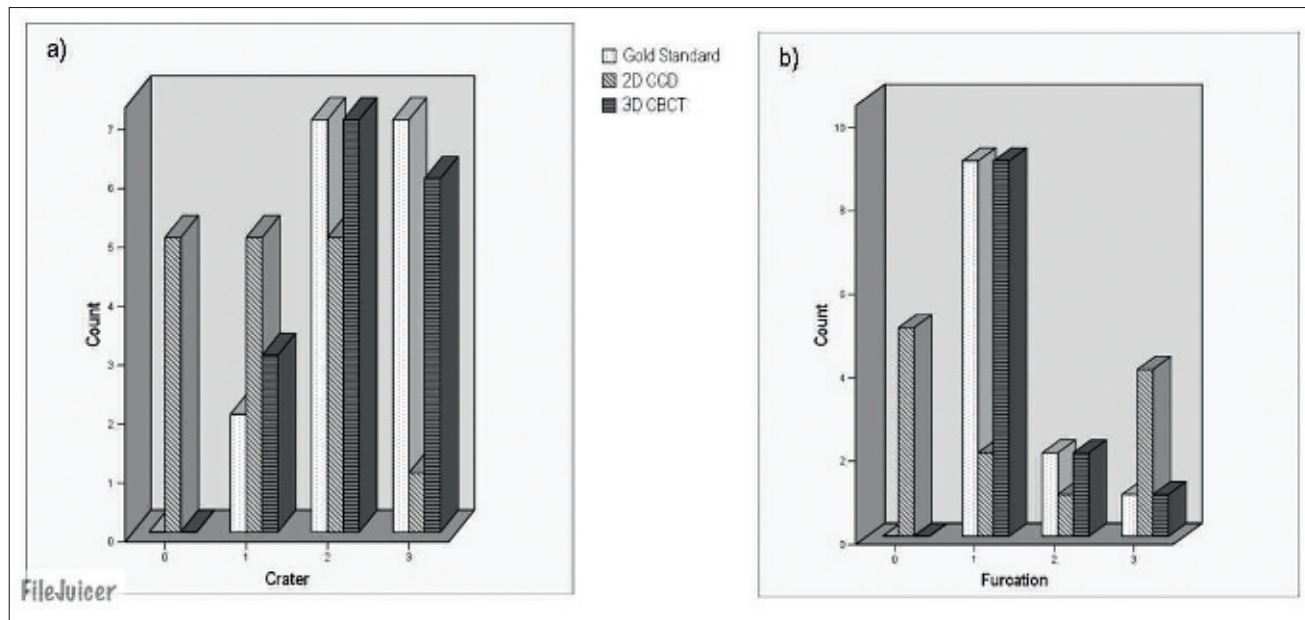


Fig 3 Bar charts of the averaged observer data showing frequency counts of the gold standard, the 2D CCD and the 3D CBCT images. a) Crater classification (0 = no defect, 1 = 1-walled, 2 = 2-walled and 3 = 3-walled); b) furcation classification (0 = no involvement, 1 = class I, 2 = class II and 3 = class III). Both graph show more precise classifications using CBCT as the frequency counts lie close to the gold standard. It can be seen that for 2D CCD images, some craters and furcation involvements were not detected.

TABLE 4. Chi-square (χ^2) tests of both variables show that there were significant differences between 2D CCD image and the gold standard, as well as between 2D CCD and 3D CBCT in assessment of craters and furcation involvements. No significant difference between 3D CBCT and the gold standard was found

		GS vs 2D CCD	GS vs 3D CBCT	2D CCD vs 3D CBCT
Crater	χ^2 value	11.119	0.277	16.250
	Df	3	2	6
	Exact Sig.	0.009	1.000	0.010
Furcation	χ^2 value	11.588	0.000	18.300
	Df	3	2	6
	Exact Sig.	0.006	1.000	0.003

dians of the crater data (gold standard = 2, CCD = 1 and CBCT = 2), but a constant value of 1 for the furcation involvement data. This limitation explained the unexpected results for furcation involvements and therefore further analyses including cross-tabulations and Chi-square tests of the furcation involvement data were made. Table 4 shows that based on frequency counts, a significant difference was found for the furcation involvement variable between the 2D CCD images and the gold standard ($p = 0.006$).

With intraoral CCD images, 58% of the furcation involvements were detectable. Among these, only 25% were correctly classified and the misclassification counts were as high as 75% (33% overestimations and 42% underestimations). Furthermore, it was not possible to distinguish vestibular from oral furcation involvements. For CBCT, 100% of the furcation involvements were visible and they were all correctly classified. Based on these frequency counts, no significant difference was found ($p = 1.000$; Table 4) between the gold standard and

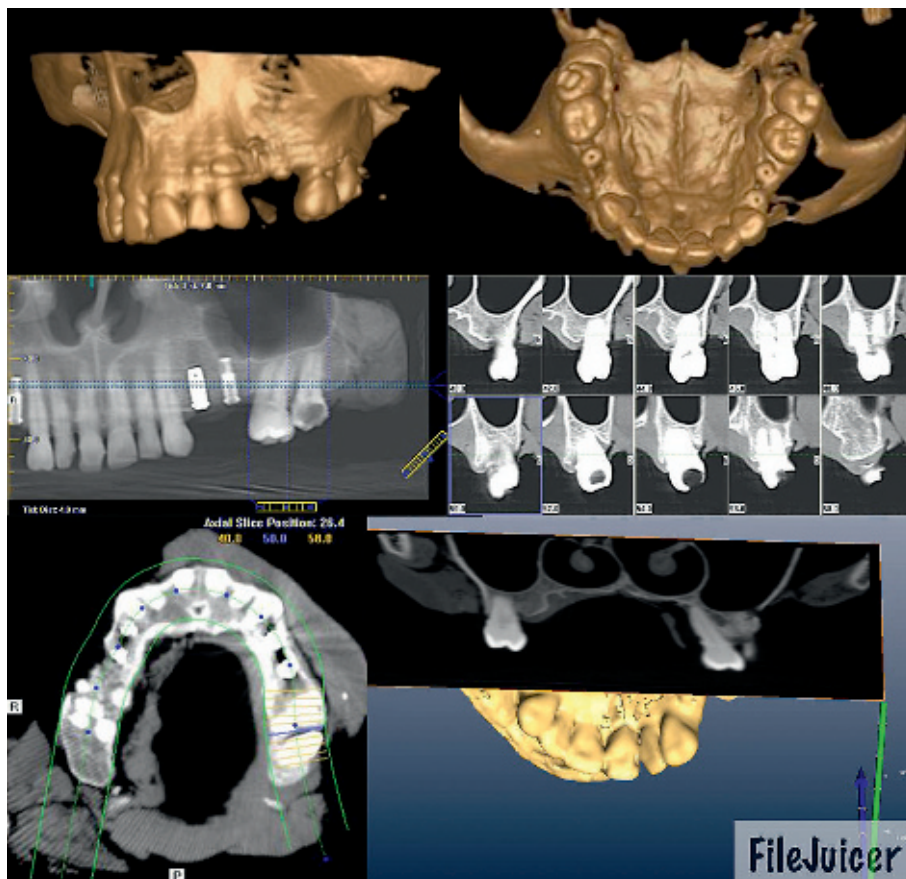


Fig 4 Three-dimensional reconstruction images of the same molar region as in Fig 2, using different software packages.

3D CBCT images in assessment of furcation involvements.

Discussion

The recent attention for CBCT requires validation of this technology for diagnostic purposes. For periodontal diagnosis, the present results revealed a better depiction of bone craters and furcation involvements from CBCT than from intraoral images. Also, vestibular and oral bone defects, as well as maxillary trifurcations, were easily assessed by CBCT images. The maxillary trifurcations are difficult to see on intraoral images, despite multiple efforts to optimise the diagnostic value of the 2D images. In the present study only 69% of the crater defects and 58% of the furcation involvements were identified from the intraoral CCD images. In contrast, there was 100% detection of both defects on CBCT. These findings are comparable with previous studies. Misch et al¹⁴ found that only 67% of the artificially created infra-bony defects were diagnosed on intraoral im-

ages. Fuhrmann et al⁹ found that 21% of artificial furcation involvements were identified on dental radiographs, and 100% through high resolution CT.

Certainly this more accurate assessment by CBCT is mainly due to the fact that CT technology provides multi-planar slices and 3D information. The innovative cone beam technology of this imaging technique additionally allows lower radiation doses, which will further increase its usage. The radiation dose of CBCT was reported to be up to 15 times lower than conventional CT²⁷. Recent studies reported that CBCT systems only require 4 to 15 times the dose of standard panoramic images²⁶, or only the dose of a film-based full mouth radiographic examination (FMX)²⁷. An FMX in the USA varies from 18 to 22 intraoral radiographs with a dose range of 13–100 μSv ^{32,33}. Effective dose of CBCT, starting at 36.9 μSv , was within the range of the FMX^{26,27}. Furthermore, Ludlow et al²⁶ reported on dose reduction when using smaller FOV examinations. Since the radiation dose of CBCT is lower than conventional CT, there is growing concern of over-use of CBCT

and its radiation safety. In the authors' opinion, the use of CBCT should still be carefully justified (diagnostic benefit and risk are balanced) and the 'as low as reasonably achievable' (ALARA) principle should be followed. In the present study, a low dose protocol of CBCT (23.87 mAs and 0.4 mm voxel size) was used. More studies with larger sample sizes should determine ideal exposure settings, which will optimise the image quality and lower the radiation exposure further.

Currently used software of CBCT requires a certain amount of experience for optimal assessment of anatomical features. The growing possibility of real 3D reconstruction of the CBCT images by more precise algorithms will further improve this by making it easier to interpret the three dimensions of crater and furcation involvements. Fig 4 shows 3D reconstruction images and manipulations of one of the selected regions (see Fig 2) on the cadaver jaws.

In the present study, we confirmed the hypothesis that CBCT would allow more accurate assessment of the periodontal bone defects than intraoral radiography. Dedicated periodontal filtering may aid bone level measurements but not craters and furcation assessments. When compared with CBCT, digital intraoral radiography is still a 2D technique with limitation of presenting 3D periodontal defects, particularly with regard to the buccal and lingual aspects of bone loss¹⁻³. Our observers were not able to distinguish vestibular from oral bony defects and detect the maxillary trifurcations by using 2D images.

While the use of digital intraoral radiography has not been found to be superior to conventional radiography for periodontal linear measures²⁰, it cannot be ignored that it offers at least two essential benefits: radiation dose reduction and image analysis for improved bone diagnostics^{34,35}. With regard to the first benefit, we attempted to reduce the intraoral radiographic dose as much as possible while keeping full diagnostic capabilities. The methods and exposure settings used in the present study have been tested and validated in our previous report¹⁵. The second benefit of digital intraoral images may allow for image optimisation and quantification, such as contrast enhancement, periodontal filtering³² and digital subtraction^{7,11,12,34,35}. These dynamic functions may aid periodontal diagnosis. Nonetheless, it is widely accepted that the 2D nature of the images, whether they are conventional or digital, prevents a diagnosis of the entire spatial bone defect. A 3D diagnosis has the potential for better assessment of prognosis of individual teeth, thus providing more efficient treatment planning.

In the preceding part of this study, measurements of linear bone loss using CBCT images were found to be

similar to intraoral CCD assessment¹⁵. However, because of the lower resolution, CBCT were scored lower than the intraoral images for bone quality and delineation of lamina dura. This indicated that the current CBCT system could not replace intraoral radiography for periodontal assessment. A combination of both imaging modalities could benefit periodontal bone assessment and assist pre-surgical treatment planning. We therefore suggest that the currently tested model of CBCT should only be used for relatively complex periodontal treatment planning, such as surgery of complex periodontal defects and the potential use of dental implants.

All observations in this study were made using a general classification system. Periodontal defects were given the general name of crater and classified as 1-walled, 2-walled, 3-walled or 4-walled in the most apical depth of the lesions. Therefore, the common classification proposed by Karn et al³⁶ was followed, avoiding the sometimes difficult nomenclature of crater, trench, moat, ramp, plane, or combinations of these. Furcation involvements were classified by looking at the horizontal component proposed by Hamp et al³⁷ (class I, II and III) and the vertical component proposed by Tarnow et al³⁸ (subclass A, B and C). As there is discrepancy of the assigned ordinal data to this scale, only the main classes were used for the statistical analyses. The classification proposed by Rosenberg et al³⁹ for maxillary trifurcations was not included as the three bifurcations were assessed separately. Most of these classifications could have been based on clinical, surgical or 2D radiological information.

Finally, validation of these imaging modalities has been achieved by comparison of detectability of anatomical or pathological features, but the ultimate test would be how much these features affect treatment decisions and treatment outcome. Therefore, further long-term clinical studies are required.

Conclusions

CBCT allowed more accurate assessment of bone craters and furcation involvements than digital intraoral radiography. This study might help in establishing selection criteria for different imaging modalities in assessment of periodontal bone loss and further assist in periodontal diagnosis and treatment planning.

Acknowledgements

We would like to thank Roslyn Gorin, MS, Statistical Application Manager, Department of Computer Sciences, Temple University, Philadelphia, USA, for her assistance with the statistical analyses.

References

1. Eickholz P, Hausmann E. Accuracy of radiographic assessment of interproximal bone loss in intrabony defects using linear measurements. *Eur J Oral Sci* 2000;108:70-73.
2. Schliephake H, Wichmann M, Donnerstag F, Vogt S. Imaging of peri-implant bone levels of implants with buccal bone defects. *Clin Oral Implants Res* 2003;14:193-200.
3. Zulqarnain BJ, Almas K. Effect of x-ray beam vertical angulation on radiographic assessment of alveolar crest level. *Indian J Dent Res* 1998;9:132-138.
4. Brägger U. Radiographic parameters: biological significance and clinical use. *Periodontol* 2000 2005;39:73-90.
5. Mol A. Imaging methods in periodontology. *Periodontol* 2000 2004;34:34-48.
6. Benn DK. A review of the reliability of radiographic measurements in estimating alveolar bone changes. *J Clin Periodontol* 1990;17:14-21.
7. Jeffcoat MK, Reddy MS. Advances in measurements of periodontal bone and attachment loss. *Monogr Oral Sci* 2000;17:56-72.
8. Muller HP, Eger T. Furcation diagnosis. *J Clin Periodontol* 1999;26:485-498.
9. Fuhrmann RA, Buckner A, Diedrich PR. Furcation involvement: comparison of dental radiographs and HR-CT-slices in human specimens. *J Periodontol Res* 1997;32:409-418.
10. Tugnait A, Clerehugh V, Hirschmann PN. The usefulness of radiographs in diagnosis and management of periodontal diseases: a review. *J Dent* 2000;28:219-226.
11. Young SJ, Chaibi MS, Graves DT, Majzoub Z, Boustany F, Cochran D, Nummikoski P. Quantitative analysis of periodontal defects in a skull model by subtraction radiography using a digital imaging device. *J Periodontol* 1996;67:763-769.
12. Cury PR, Araujo NS, Bowie J, Sallum EA, Jeffcoat MK. Comparison between subtraction radiography and conventional radiographic interpretation during long-term evaluation of periodontal therapy in Class II furcation defects. *J Periodontol* 2004;75:1145-1149.
13. Deas DE, Moritz AJ, Mealey BL, McDonnell HT, Powell CA. Clinical reliability of the "furcation arrow" as a diagnostic marker. *J Periodontol* 2006;77:1436-1441.
14. Misch KA, Yi ES, Sarment DP. Accuracy of cone beam computed tomography for periodontal defect measurements. *J Periodontol* 2006;77:1261-1266.
15. Vandenberghé B, Jacobs R, Yang J. Diagnostic validity (or acquity) of 2D CCD versus 3D CBCT-images for assessing periodontal breakdown (in press).
16. Almog DM, LaMar J, LaMar FR, LaMar F. Cone beam computerized tomography-based dental imaging for implant planning and surgical guidance, Part 1: Single implant in the mandibular molar region. *J Oral Implantol* 2006;32:77-82.
17. Guerrero ME, Jacobs R, Loubele M, Schutyser F, Suetens P, van Steenberghe D. State-of-the-art on cone beam CT imaging for preoperative planning of implant placement. *Clin Oral Investig* 2006;10:1-7.
18. Eickholz P, Riess T, Lenhard M, Hassfeld S, Staehle HJ. Digital radiography of interproximal bone loss; validity of different filters. *J Clin Periodontol* 1999;26:294-300.
19. Kobayashi K, Shimoda S, Nakagawa Y, Yamamoto A. Accuracy in measurement of distance using limited cone-beam computerized tomography. *Int J Oral Maxillofac Implants* 2004;19:228-231.
20. Pecoraro M, Azadivatan-le N, Janal M, Khocht A. Comparison of observer reliability in assessing alveolar bone height on direct digital and conventional radiographs. *Dentomaxillofac Radiol* 2005;34:279-284.
21. Paurazas SB, Geist JR, Pink FE, Hoen MM, Steinman HR. Comparison of diagnostic accuracy of digital imaging by using CCD and CMOS-APS sensors with E-speed film in the periapical bony lesions. *Oral Surg Oral Med Oral Pathol Oral Radiol Endod* 2000;89:356-362.
22. Kaeppler G, Vogel A, Axmann-Krcmar D. Intra-oral storage phosphor and conventional radiography in the assessment of alveolar bone structures. *Dentomaxillofac Radiol* 2000;29:362-367.
23. Muller HP, Eger T, Lange DE. Management of furcation-involved teeth. A retrospective analysis. *J Clin Periodontol* 1995;22:911-917.
24. Svardstrom G, Wennstrom JL. Periodontal treatment decisions for molars: an analysis of influencing factors and long-term outcome. *J Periodontol* 2000;71:579-585.
25. Tsiklakis K, Donta C, Gavala S, Karayianni K, Kamenopoulou V, Hourdakos CJ. Dose reduction in maxillofacial imaging using low dose Cone Beam CT. *Eur J Radiol* 2005;56:413-417.
26. Ludlow JB, Davies-Ludlow LE, Brooks SL, Howerton WB. Dosimetry of 3 CBCT devices for oral and maxillofacial radiology: CB Mercuray, NewTom 3G and I-CAT. *Dentomaxillofac Radiol* 2006;35:219-226.
27. Scarfe WC, Farman AG, Sukovic P. Clinical applications of cone beam computed tomography in dental practice. *J Can Dent Assoc* 2006;72:75-80.
28. Jacobs R, Adriansens A, Verstreken K, Suetens P, van Steenberghe D. Predictability of a three-dimensional planning system for oral implant surgery. *Dentomaxillofac Radiol* 1999;28:105-111.
29. White DR. Phantom materials for photons and electrons. The Hospital Physicists' Association, Radiotherapy Topic Group. *Scientific Report Series* 1977;20:1-30.
30. Afifi AA, Clark V. Computer aided multivariate analysis, 2nd edition. California: Lifetime Learning Publications, 1984.
31. Siegel S. Non parametric statistics for the behavioural sciences. New York: McGraw-Hill, 1956.
32. Gibbs SJ. Effective dose equivalent and effective dose: comparison for common projections in oral and maxillofacial radiology. *Oral Surg Oral Med Oral Pathol Oral Radiol Endod* 2000;90:538-545.
33. White SC. 1992 assessment of radiation risk from dental radiography. *Dentomaxillofac Radiol* 1992;21:118-126.
34. Mol A. Image processing tools for dental applications. *Dent Clin North Am* 2000;44:299-318.
35. van der Stelt PF. Principles of digital imaging. *Dent Clin North Am* 2000;44:237-248.
36. Karn KW, Shockett HP, Moffitt WC, Gray JL. Topographic classification of deformities of the alveolar process. *J Periodontol* 1984;55:336-340.
37. Hamp SE, Nyman S, Lindhe J. Periodontal treatment of multirooted teeth. Results after 5 years. *J Clin Periodontol* 1975;2:126-135.
38. Tarnow D, Fletcher P. Classification of the vertical component of furcation involvement. *J Periodontol* 1984;55:283-284.
39. Rosenberg MM. Management of osseous defects, furcation involvements, and periodontal-pulpal lesions. In: Clark JW (ed). *Clinical Dentistry: Periodontal and Oral Surgery Vol 10*. Philadelphia: Harper and Row, 1985:108-117.